Hindawi Publishing Corporation
Shock and Vibration
Volume 2016, Article ID 1276753, 8 pages
http://dx.doi.org/10.1155/2016/1276753

Research Article

Nonlinear Modeling and Identification of an Aluminum Honeycomb Panel with Multiple Bolts

Yongpeng Chu, Hao Wen, and Ti Chen

State Key Laboratory of Mechanics and Control of Mechanical Structures, Nanjing University of Aeronautics and Astronautics, 29 Yudao Street, Nanjing, Jiangsu 210016, China

Correspondence should be addressed to Hao Wen; wenhao@nuaa.edu.cn

Received 20 September 2016; Accepted 27 November 2016

Academic Editor: Sumeet S. Aphale

This paper focuses on the nonlinear dynamics modeling and parameter identification of an Aluminum Honeycomb Panel (AHP) with multiple bolted joints. Finite element method using eight-node solid elements is exploited to model the panel and the bolted connection interface as a homogeneous, isotropic plate and as a thin layer of nonlinear elastic-plastic material, respectively. The material properties of a thin layer are defined by a bilinear elastic plastic model, which can describe the energy dissipation and softening phenomena in the bolted joints under nonlinear states. Experimental tests at low and high excitation levels are performed to reveal the dynamic characteristics of the bolted structure. In particular, the linear material parameters of the panel are identified via experimental tests at low excitation levels, whereas the nonlinear material parameters of the thin layer are updated by using the genetic algorithm to minimize the residual error between the measured and the simulation data at a high excitation level. It is demonstrated by comparing the frequency responses of the updated FEM and the experimental system that the thin layer of bilinear elastic-plastic material is very effective for modeling the nonlinear joint interface of the assembled structure with multiple bolts.

1. Introduction

In the aeronautical and aerospace fields, a much more attention has been attracted by the assembled mechanical structures which consist of substructures or parts connected to each other through different types of connections [1–5]. If the effects of the mechanical joints on the dynamics are neglected in the model of the mechanical structures, there may exist a significant error between the theoretical and experimental results, especially in some cases having large excitation or motion levels [6]. The main reason is that most of the structure connections may cause the change of stiffness and damping. However, due to the complex dynamics characteristics of the assembled structures, it is difficult and challenging to model these structures accurately. An accurate model for joints is the key to the success of the dynamic analysis of assembled structures. Many researchers have focused on how to resolve such a problem using the theoretical or experimental methods [7–10]. For instance, Kuether and Allen presented two model substructuring techniques for describing the nonlinear dynamic behavior of an assembled structure [11]. Hammami et al. [12] presented a detailed review on the damping design of a jointed structure. Segalman [13] investigated a four-parameter model for lap-type joints to capture the dissipation behavior of harmonically loaded experiments. Bograd et al. [14] gave an overview of various joint types, their characteristics, and the models used for their simulation as well as an extensive information of up-to-date literature associated with this topic. Jalali et al. [15] studied the weakly nonlinear systems of multiple degrees of freedom by describing functions inversion. Morelli [16] developed a new method for the structures to identify transfer function models from the noisy data. Marinone et al. [17] proposed a model modification response technique for computing the time response of a nonlinear system. Peter et al. [18] presented an integrated method for estimating linear as well as nonlinear system parameters of a structure based on its nonlinear normal modes (NNMs) and performed the Harmonic Balance Method (HBM) to numerically calculate the NNMs.

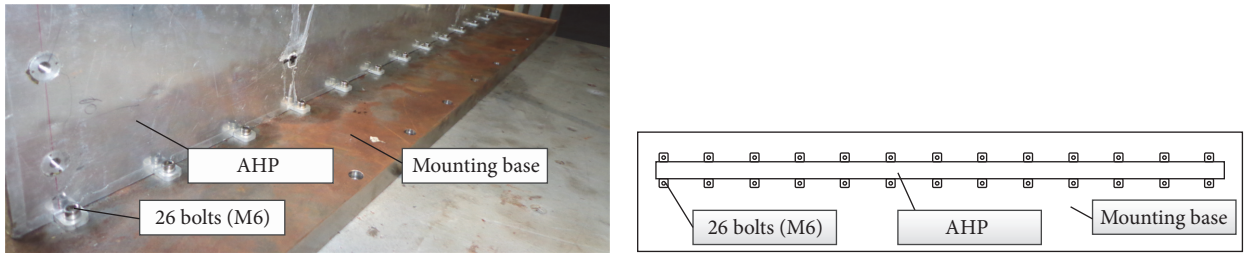

(a) (b)

Figure 1: (a) The AHP connected to a mounting base via multiple bolts. (b) A graphic illustration of the bolted connections.

Among the mechanical connections, bolted joints are applied in assembled mechanical structures very frequently. A number of researchers have paid attention in developing predictive models for bolted joints in different structures. For example, Song et al. [19] developed an adjusted Iwan model approach to simulate the nonlinear dynamic behavior of bolted joints in beam structures. Jalali et al. [20] presented a nonlinear model possessing a single degree of freedom in order to describe the governing equation of bolted joints interface between two beams. Ahmadian and Jalali [4] used a nonlinear spring to represent the softening phenomenon of the joint interface in the modeling of the joint which was in the mid span of an Euler–Bernoulli beam. Li et al. [21] proposed an identification method for the bolted joint in a cantilever beam of steel. Yang et al. [22] derived the identification equations and identified the joint parameters in the assemble beam by using the substructural synthesis method. Luan et al. [23] proposed a simplified nonlinear dynamic model, in which the mechanical properties of the bolted joint in a flange assembled structure were modeled by bilinear springs. Mayer and Gaul [24] studied the modeling of the nonlinear stiffness and damping mechanisms between jointed members in the built-up structures and showed a comparison between two different segment-to-segment contact elements, that is, the so-called TLEs and zero thickness elements.

It is noted that the previous researches mainly focused on the assembled structures consisting of several beams, pipes, or other simple parts connected through a small amount of bolts. Finite Element Models (FEMs) have been developed to describe the dynamic phenomena of assembled structures by treating each connected interface as a thin layer of a nonlinear elastic-plastic material [25–27]. It has been demonstrated that a thin layer of a nonlinear material is effective to describe the nonlinearity due to bolted connections. Alamdari et al. [26] utilized a thin layer of solid elements to model the joint interface between two pipes. Iranzad and Ahmadian [27] adopted a thin layer interface model of virtual elastic plastic material to simulate nonlinear effect of bolted joints in the beams.

It is to be noted here that less attention has been given to model the panel structure with multiple bolted connections although much of the literature focused on modeling of the bolted beams and pipes. The aim of this work is to study the nonlinear dynamics modeling and parameter identification of an AHP with multiple bolted joints. For this purpose, a thin layer of nonlinear elastic-plastic material is used to characterize the nonlinear characteristics of the bolted connection interface. The linear material parameters of the panel are necessarily identified via experimental tests at low excitation levels, whereas the nonlinear material parameters of the thin layer are updated by using the genetic algorithm to minimize the residual error between the measured and the simulation data at a high excitation level. Finally, the efficacy of the proposed scheme is demonstrated via comparisons of the FEM and experimentally obtained results under another exciting level.

2. Nonlinear Dynamics Modeling

As shown in Figure 1, this study is concerned with the assembled structure consisting of an AHP and a mounting base connected to each other via multiple bolts. The AHP has a length of 1000 mm, a width of 1000 mm, and a thickness of 30 mm. The volume and weight of the AHP are 0.03 m^3 and 5.80 kg, respectively. The AHP is fixed at the bottom by using 26 bolts (13 bolts for each side). The pretightening torque of the bolts is set to be about 2 Nm.

The nonlinear characteristics of the bolted joints, such as micro/macroslip, may have a significant effect on the dynamical behavior of assembled structures. Therefore, it is of practical importance to accurately model the nonlinear characteristics of the bolted joints interface. The equation of motion for a nonlinear system with multiple degrees of freedom under harmonic excitation can be expressed as follows [28]:

$$\mathbf{M}\ddot{\mathbf{x}} + \mathbf{C}\dot{\mathbf{x}} + \mathbf{K}\mathbf{x} + \mathbf{F}_{\mathbf{NL}}(\mathbf{x}, \dot{\mathbf{x}}) = \mathbf{f} \sin \omega t, \tag{1}$$

where $\mathbf{x}$ and $\dot{\mathbf{x}}$ are the vectors of displacements and velocities, $\mathbf{F}_{\mathbf{NL}}(\mathbf{x}, \dot{\mathbf{x}})$ represents the nonlinear internal force which is a function of the displacements and velocities, $\mathbf{f}$ is the amplitude vector of the excitation forces, ω is the excitation frequency, and $\mathbf{M}$, $\mathbf{C}$, and $\mathbf{K}$ denote the mass, damping, and stiffness matrix, respectively.

Quite different from the cases of linear systems, it is well known that the frequency response of such a nonlinear system depends on the levels of the excitation forces due to the presence of the nonlinear internal force. In this study, the finite element method is adopted to model the assembled

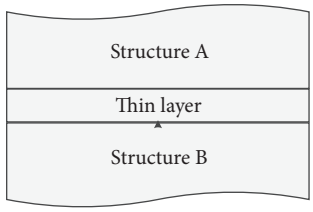

Figure 2: The sketch of the thin layer of elastic-plastic material.

structure where the connection interface with multiple bolts is treated as a thin layer of bilinear elastic-plastic material so as to characterize the nonlinear behavior of the bolted joints. Figure 2 shows a sketch of the thin layer which connects Structure A (the AHP) to Structure B (the mounting base).

The thickness of the thin layer is much less than the geometric sizes in the other two directions. Following [24], the following assumptions are considered to model the constitutive relation of the thin layer. The thickness of the thin layer element is approximately equal to zero; consequently, the normal contact behavior of thin layer element is decoupled from the tangential behavior. Take the case of linear material, for example. The constitutive relation of the thin layer element can be written as [24]

$$\begin{Bmatrix} u_n \\ u_{Tx} \\ u_{Ty} \end{Bmatrix} = \begin{bmatrix} c_{11} & 0 & 0 \\ 0 & c_{55} & 0 \\ 0 & 0 & c_{66} \end{bmatrix} \begin{Bmatrix} \xi_n \\ \varsigma_{Tx} \\ \varsigma_{Ty} \end{Bmatrix}, \tag{2}$$

where n, x, and y represent the contact normal and the local x- and y-tangential directions, respectively; u_n and ξ_n represent the normal stress and strain component of the interface; u_{Tx} and u_{Ty} represent the tangential stress; and ς_{Tx} and ς_{Ty} represent the tangential strain. In the case of linear material, c_{11} denotes Young's modulus, and $c_{55} = c_{66}$ is the shear modulus, which can describe the normal and tangential stiffness of the thin layer element.

In the case of the nonlinear material, the constitutive relation has a more complex form. In this study, a bilinear elastic-plastic model under the assumption of isotropic hardening and Von Mises yield criterion is used to describe the stress-strain relationship of a thin layer element [29]. Elastic-plastic behavior of an isotropic hardening is described by using the three parameters, that is, Young's modulus, yielding point, and hardening modulus. Figure 3 shows the bilinear stress-strain behavior for one-dimensional uniaxial case [30], where the material initially deforms with Young's modulus E_e as its slope, until the stress level reaches the uniaxial yield stress S_Y, and then the behavior of material can be described by using hardening modulus E_p.

As shown in Figure 3, E_e, S_Y, and E_p represent Young's modulus, yield stress, and hardening modulus, respectively. In the case of one-dimensional uniaxial case, the constitutive equation can be written as

$$\begin{aligned} \sigma &= E_e \varepsilon \quad \varepsilon \le \varepsilon_s, \\ \sigma &= S_Y + E_p (\varepsilon - \varepsilon_s) \quad \varepsilon > \varepsilon_s, \end{aligned} \tag{3}$$

where σ is the stress and ε is the strain.

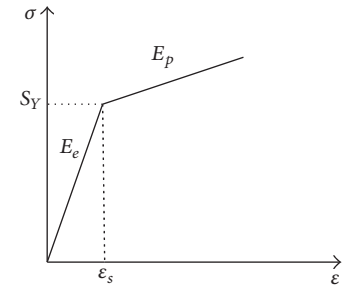

Figure 3: Bilinear stress-strain behavior for one-dimensional space.

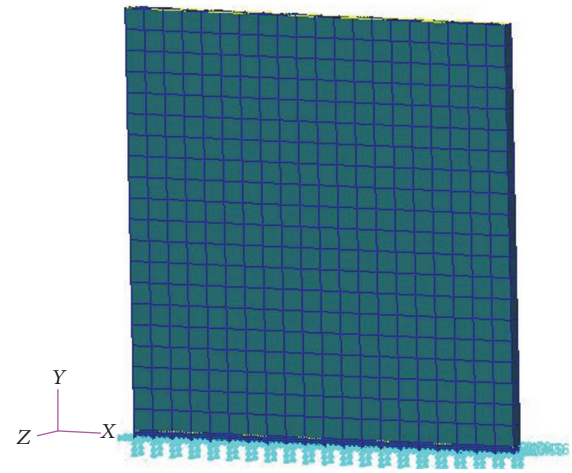

Figure 4: The FEM of the assembled structure.

The FEM of the AHP with multiple bolts is created in *MSC/NASTRAN* [29]. Figure 4 shows the FEM of the structure. Eight-node solid elements are adopted to create the AHP. The material of the model is assumed to be an isotropic and described using three material parameters, that is, Young's modulus, Poisson's ratio, and shear modulus. The elastic-plastic material properties of the thin layer can be defined by using MAT1 and MAST1 cards of *NASTRAN*. The thickness of the thin layer is selected by considering the following dimensionless parameter:

$$\gamma = \frac{\max(l_1, l_2)}{d}, \tag{4}$$

where l_1 and l_2 are length and width of the thin layer element and d is the thickness of the thin layer element. To facilitate numerical computation, it is suggested by [31] to select $\gamma \in [10, 100]$. In this work, the thickness of the thin layer is chosen such that $\gamma = 100$.

3. Model Identification

In the FEM of the assembled structure, the AHP is treated as a linear plate of homogeneous, isotropic material. The mass density of the plate is determined using the volume and weight of the AHP. The equivalent Young's modulus and Poisson's ratio are set to be guessed values and then updated by using the SOL200 procedure in NASTRAN to minimize

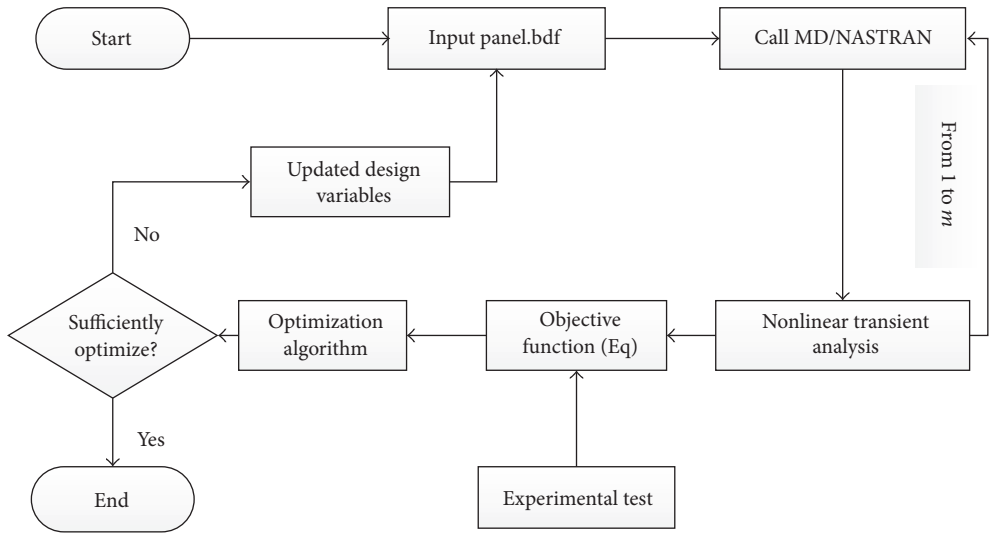

Figure 5: Flowchart of the optimization procedure.

the error between the first three-order natural frequencies of FEM and real structure. Accordingly, the objective function can be expressed as follows:

$$\text{Objective} = \min \quad \sum_{i=1}^{3} \kappa_i \left[\frac{\left(\omega_i^{\text{FEM}} - \omega_i^{\text{Test}}\right)}{\omega_i^{\text{Test}}} \right]^2, \tag{5}$$

where ω_i^{FEM} and ω_i^{Test} are numerically and experimentally obtained ith order natural frequencies and κ_i is the weight coefficient. It is noteworthy that the location and magnitude of the applied exciting forces are identical with those in the experimental test.

Moreover, the nonlinear material parameters of the thin layer, that is, Young's modulus E_e, yielding point S_Y, and hardening modulus E_p, are updated by minimizing the error between the responses of numerical simulation based on FEM and the experimental test. The dynamic responses of the FEM with harmonic excitation are obtained in the time domain by using nonlinear transient module of NASTRAN and then transferred into the frequency domain using MATLAB programming environment. The three material parameters of the thin layer are chosen as design variables and are then updated to minimize the following objective function:

$$\text{OBJ} = \min \quad \sum_{i=1}^{m} \left\{ \left[\frac{\left(\alpha^{\text{FEM}}(\omega_i) - \alpha^{\text{Test}}(\omega_i)\right)}{\alpha^{\text{Test}}(\omega_i)} \right] \right\}^2, \tag{6}$$

where $\alpha^{\text{FEM}}(\omega_i)$ and $\alpha^{\text{Test}}(\omega_i)$ are numerical and experimental responses and m is the number of the selected frequency points. In other words, the objective function of (6) is a measure of the difference between numerical and experimental responses in the frequency domain. The nonlinear optimization problem can be cast as finding $\mathbf{X}$ so as to minimize the objective function $F(\mathbf{X})$ subject to possible inequality and equality constraints:

$$\begin{aligned} &\text{Objective: } F(\mathbf{X}) \\ &g_j(\mathbf{X}) \le 0 \quad j = 1, \ldots, n_g, \text{ inequality constraints,} \\ &h_k(\mathbf{X}) = 0 \quad k = 1, \ldots, n_h, \text{ equality constraints,} \\ &x_i^L \le x_i \le x_i^U \quad i = 1, \ldots, n, \text{ side constraints,} \\ &\mathbf{X} = \{x_1, x_2, \ldots, x_n\}, \text{ design variables.} \end{aligned} \tag{7}$$

It is worthy to note here that the parameter updating of the thin layer material is nonlinear by nature and cannot be solved using the off-the-shell modules in NASTRAN. Thus, the genetic algorithm optimizer of MATLAB is used for the optimization task through the real-time data exchange with the NASTRAN. Figure 5 depicts the main procedure of the optimization task: an input file (panel.bdf) with model information is generated using a preprocessing modeling software, and then NASTRAN is called with the input file for a series of nonlinear transient analyses of the structure subject to exciting forces with different frequencies; the dynamic responses obtained using NASTRAN and experimental testing are converted into the frequency domain through the application of the fast Fourier transform method; the genetic algorithm optimizer of MATLAB takes the frequency response data for the instantaneous computation of the objective function and the constraints and updates the design variables, namely, E_e, S_Y, and E_p, so as to reduce the constraint violation or to improve the performance index until a prespecified optimization criterion is satisfied.

4. Experimental Studies

Experimental test was conducted to investigate the dynamic characteristics of the AHP with multiple bolts. The testing system setup mainly consists of an electromagnetic vibration

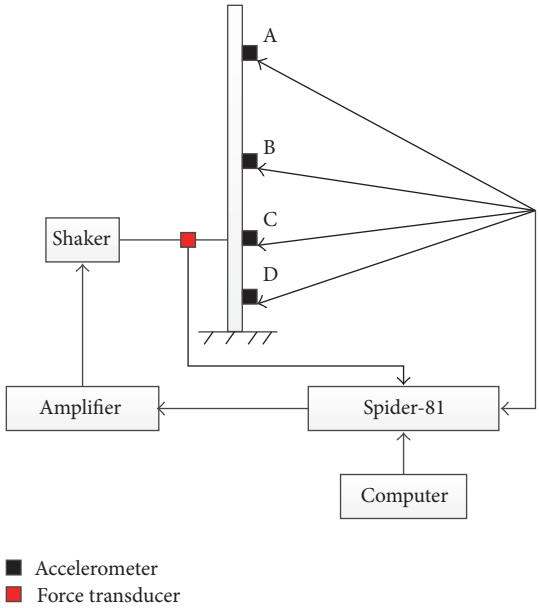

Figure 6: A schematic view of the experimental setup.

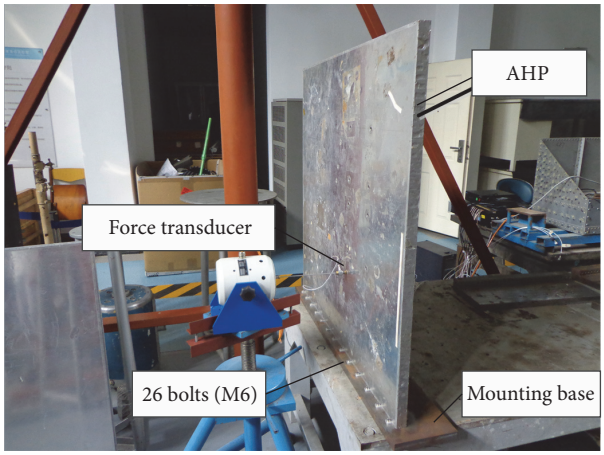

Figure 7: Experimental system for vibration test of the AHP with multiple bolts.

exciter (S 51075-M from TIRA GmbH), a power amplifier (B&K2718 from Brüel & Kjær), and a vibration test controller (Spider-81 from Crystal Instruments), as shown in Figure 6. The input force and the dynamic responses of the system are measured using a force transducer (208C02 from PCB Piezotronics) and four acceleration sensors (333B52 from PCB Piezotronics), respectively, as shown in Figures 6 and 7.

Two different stages of experimental tests were carried out. In the first part, the AHP is excited by using random excitation (RMS 1×10^{-4}) and sinusoidal forces (0.5 N), respectively. The excitation time is set in the Spider-81 software system to be 10 minutes. Figure 8 describes the data of Frequency Response Function (FRF) acquired at sensor location A using the Engineering Data Management (EDM) software from Crystal Instruments. The experimental results obtained using the random and the sinusoidal excitations at

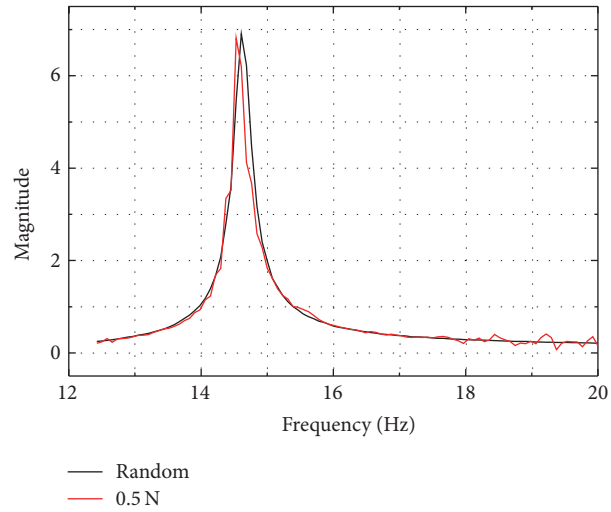

Figure 8: Measured linear FRF at sensor location A.

Table 1: Measured first three natural frequencies.

Order number	1	2	3
Natural frequency (Hz)	14.63	104.02	144.40

a small level are almost the same to each other since the assembled structure behaves linearly in the case of small excitation level. In addition, Table 1 gives the first three natural frequencies of the assembled structure obtained using the linear tests. The first group of the tests are performed for the linear identification of the AHP parameters, where the AHP is treated as a clamped plate of homogeneous, isotropic material.

The linear material parameters of AHP are updated by minimizing the objective function defined as (5) by using SOL 200 procedure of NASTRAN. The initial values of Young's modulus and Poisson's ratio are taken to be 4.50 Gpa and 0.33, respectively. Figures 9–11 show the variations of the objective function and the design parameters with the design cycles in the optimization process, respectively. Table 2 shows the updated results of material parameters and Table 3 shows the experimentally measured, initially estimated, and updated natural frequencies.

In the second part, the AHP was excited using sinusoidal forces at much larger levels so as to identify the nonlinear characteristics of the system. Two different levels of excitation forces (5 N and 8 N) were considered for the experimental tests with its testing frequency range set to be from 11 Hz to 15 Hz in the Spider-81 software system. Quite different from the case of a linear structure, Figure 12 shows the measured FRF and the natural frequency of the structure being decreased with the amplitude of the exciting force.

In this part, the parameters of Young's modulus E_e, yielding point S_Y, and hardening modulus E_p are updated by minimizing the objective function defined as (6). The optimization process of the nonlinear material parameters is illustrated by Figure 5 and performed using the genetic algorithm optimizer of MATLAB through the real-time

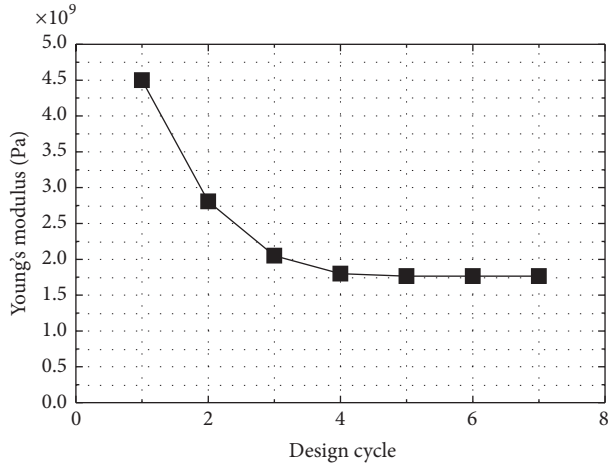

Figure 9: Variation of Young's modulus with the design cycles.

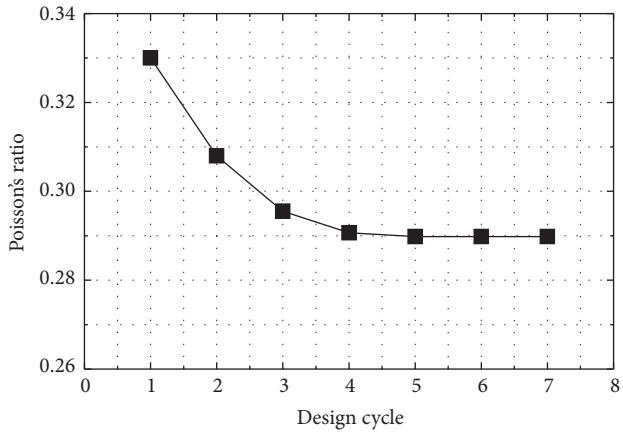

Figure 10: Variation of Poisson's ratio with the design cycles.

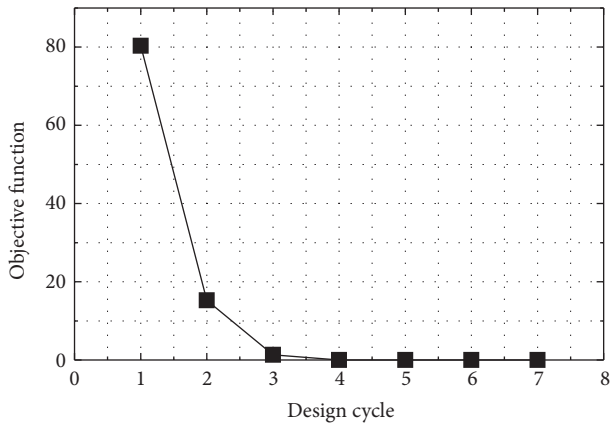

Figure 11: Variation of the objective function with the design cycles.

data exchange with the NASTRAN solver. The results of optimization are shown in Table 4 and Figures 13 and 14. The responses of the updated FEM model well coincide with that of the experimentally measured responses, as shown in Figure 13. Finally, the proposed strategy is verified by comparing the frequency responses of the updated model

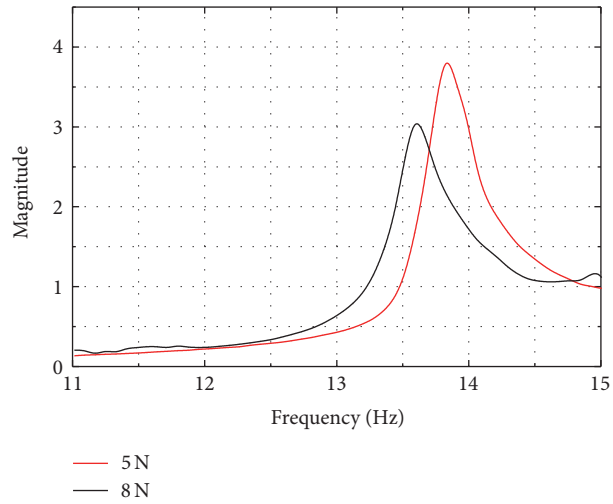

Figure 12: Measured nonlinear FRF at sensor location A.

Table 2: Initial and updated material parameters.

Material parameters	Initial value	Updated value
E (Pa)	4.50e9	1.76e9
μ	0.33	0.29

Table 3: Experimentally measured, initial, and updated natural frequencies.

Natural frequency	Experimental value	Initial value	Updated value
f_1	14.63	23.6	14.63
f_2	104.02	149.38	102.86
f_3	144.40	189.89	137.62

Table 4: Updated parameters of the thin layer.

Parameter	E_e (Pa)	E_p (Pa)	S_Y (Pa)
Updated value	8.01e8	1.27e6	7.91e6

and the experimental test under another exciting level (8 N). Figure 14 demonstrates a remarkable agreement between the dynamic responses of the updated FEM model and the experimental test under 8 N excitation force. It confirms that the updated FEM model can well characterize the nonlinear behavior of the assembled structure with multiple bolts subject to higher levels of excitations.

5. Conclusions

The aim of this study is to investigate the nonlinear dynamics modeling and parameter identification of AHP with multiple bolts. It is shown by experimental tests that the dynamic responses of the AHP with multiple bolts under low and high excitation levels are linear and nonlinear, respectively. The equivalent linear material parameters of the panel are identified using the linear response at low excitation level. A thin layer of elastic-plastic material is used to characterize

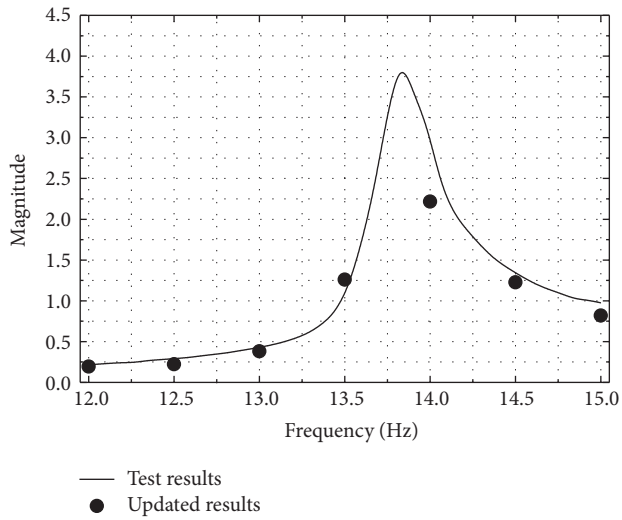

Figure 13: Measured and updated FRFs with 5 N excitation.

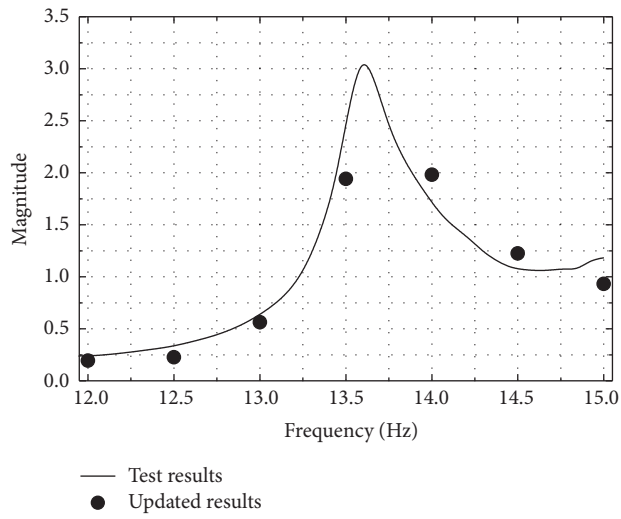

Figure 14: Measured and updated FRFs with 8 N excitation.

the bolted joints interface since the constitutive relation of such a material can describe the nonlinear behavior of the bolted interface. The parameters of nonlinear material of thin layer are updated by minimizing the error between FEM and experimentally measured results under a high excitation level. It is demonstrated that the frequency responses of the updated FEM model and experimental tests agree well with each other. The updated FEM model can be used to characterize the nonlinear behavior of the assembled structure with multiple bolts subject to higher levels of excitations.

Competing Interests

The authors declare that there is no conflict of interests regarding the publication of this paper.

Acknowledgments

This work was supported in part by the National Natural Science Foundation of China under Grants 11372130, 11290153, and 11290154 and in part by the Foundation for the Author of National Excellent Doctoral Dissertation of China under Grant 201233.

References

[1] H. Cheng, Y. Li, K.-F. Zhang, and J.-B. Su, "Efficient method of positioning error analysis for aeronautical thin-walled structures multi-state riveting," *International Journal of Advanced Manufacturing Technology*, vol. 55, no. 1–4, pp. 217–233, 2011.

[2] K. Zhang, H. Cheng, and Y. Li, "Riveting process modeling and simulating for deformation analysis of aircraft's thin-walled sheet-metal parts," *Chinese Journal of Aeronautics*, vol. 24, no. 3, pp. 369–377, 2011.

[3] O. K. Bedair and G. F. Eastaugh, "A numerical model for analysis of riveted splice joints accounting for secondary bending and plates/rivet interaction," *Thin-Walled Structures*, vol. 45, no. 3, pp. 251–258, 2007.

[4] H. Ahmadian and H. Jalali, "Identification of bolted lap joints parameters in assembled structures," *Mechanical Systems and Signal Processing*, vol. 21, no. 2, pp. 1041–1050, 2007.

[5] L. Gaul and J. Lenz, "Nonlinear dynamics of structures assembled by bolted joints," *Acta Mechanica*, vol. 125, no. 1, pp. 169–181, 1997.

[6] A. Przekop, H.-Y. T. Wu, and P. Shaw, "Nonlinear finite element analysis of a composite non-cylindrical pressurized aircraft fuselage structure," in *Proceedings of the 55th AIAA/ASMe/ASCE/AHS/SC Structures, Structural Dynamics, and Materials Conference - SciTech Forum and Exposition*, pp. 1–22, Fort Washington, MD, USA, January 2014.

[7] A. Carrella and D. J. Ewins, "Identifying and quantifying structural nonlinearities in engineering applications from measured frequency response functions," *Mechanical Systems and Signal Processing*, vol. 25, no. 3, pp. 1011–1027, 2011.

[8] M. B. Özer, H. N. Özgüven, and T. J. Royston, "Identification of structural non-linearities using describing functions and the Sherman-Morrison method," *Mechanical Systems and Signal Processing*, vol. 23, no. 1, pp. 30–44, 2009.

[9] H. Ahmadian, J. E. Mottershead, S. James, M. I. Friswell, and C. A. Reece, "Modelling and updating of large surface-to-surface joints in the AWE-MACE structure," *Mechanical Systems and Signal Processing*, vol. 20, no. 4, pp. 868–880, 2006.

[10] S. M. S. Sadati, A. S. Nobari, and T. Naraghi, "Identification of a nonlinear joint in an elastic structure using optimum equivalent linear frequency response function," *Acta Mechanica*, vol. 223, no. 7, pp. 1507–1516, 2012.

[11] R. J. Kuether and M. S. Allen, "Nonlinear modal substructuring of systems with geometric nonlinearities," in *Proceedings of the 54th AIAA/ASMe/ASCE/AHS/SC Structures, Structural Dynamics, and Materials Conference*, pp. 1–19, Boston, Mass, USA, 2014.

[12] C. Hammami, E. Balmes, and M. Guskov, "Numerical design and test on an assembled structure of a bolted joint with viscoelastic damping," *Mechanical Systems and Signal Processing*, vol. 70-71, pp. 714–724, 2016.

[13] D. J. Segalman, "A four-parameter Iwan model for lap-type joints," *Journal of Applied Mechanics*, vol. 72, no. 5, pp. 752–760, 2005.

[14] S. Bograd, P. Reuss, A. Schmidt, L. Gaul, and M. Mayer, "Modeling the dynamics of mechanical joints," *Mechanical Systems and Signal Processing*, vol. 25, no. 8, pp. 2801–2826, 2011.

[15] H. Jalali, B. T. Bonab, and H. Ahmadian, "Identification of weakly nonlinear systems using describing function inversion," *Experimental Mechanics*, vol. 51, no. 5, pp. 739–747, 2011.

[16] E. A. Morelli, "Transfer function identification using orthogonal Fourier transform modeling functions," in *Proceedings of the AIAA Atmospheric Flight Mechanics Conference (AFM '13)*, pp. 678–696, 2013.

[17] T. Marinone, P. Avitabile, J. Foley, and J. Wolfson, "Efficient computational nonlinear dynamic analysis using modal modification response technique," *Mechanical Systems and Signal Processing*, vol. 31, pp. 67–93, 2012.

[18] S. Peter, A. Grundler, P. Reuss, L. Gaul, and R. I. Leine, "Towards finite element model updating based on nonlinear normal modes," in *Nonlinear Dynamics, Volume 1: Proceedings of the 33rd IMAC, A Conference and Exposition on Structural Dynamics, 2015*, Conference Proceedings of the Society for Experimental Mechanics Series, pp. 209–217, Springer, Berlin, Germany, 2016.

[19] Y. Song, C. J. Hartwigsen, D. M. McFarland, A. F. Vakakis, and L. A. Bergman, "Simulation of dynamics of beam structures with bolted joints using adjusted Iwan beam elements," *Journal of Sound and Vibration*, vol. 273, no. 1-2, pp. 249–276, 2004.

[20] H. Jalali, H. Ahmadian, and J. E. Mottershead, "Identification of nonlinear bolted lap-joint parameters by force-state mapping," *International Journal of Solids and Structures*, vol. 44, no. 25-26, pp. 8087–8105, 2007.

[21] L. Li, A. Cai, T. Guo, and X. Ruan, "Solution of ill-posed problems for identification of the dynamic parameters of bolted joints," *Journal of Mechanical Science and Technology*, vol. 28, no. 9, pp. 3471–3481, 2014.

[22] T. Yang, S.-H. Fan, and C.-S. Lin, "Joint stiffness identification using FRF measurements," *Computers & Structures*, vol. 81, no. 28-29, pp. 2549–2556, 2003.

[23] Y. Luan, Z.-Q. Guan, G.-D. Cheng, and S. Liu, "A simplified nonlinear dynamic model for the analysis of pipe structures with bolted flange joints," *Journal of Sound and Vibration*, vol. 331, no. 2, pp. 325–344, 2012.

[24] M. H. Mayer and L. Gaul, "Segment-to-segment contact elements for modelling joint interfaces in finite element analysis," *Mechanical Systems and Signal Processing*, vol. 21, no. 2, pp. 724–734, 2007.

[25] Y. Zhao, C. Yang, L. Cai, W. Shi, and Z. Liu, "Surface contact stress-based nonlinear virtual material method for dynamic analysis of bolted joint of machine tool," *Precision Engineering*, vol. 43, pp. 230–240, 2016.

[26] M. M. Alamdari, J. Li, B. Samali, H. Ahmadian, and A. Naghavi, "Nonlinear joint model updating in assembled structures," *Journal of Engineering Mechanics*, vol. 140, no. 7, Article ID 04014042, 2014.

[27] M. Iranzad and H. Ahmadian, "Identification of nonlinear bolted lap joint models," *Computers & Structures*, vol. 96-97, pp. 1–8, 2012.

[28] M. Aykan and H. N. Özgüven, "Parametric identification of nonlinearity in structural systems using describing function inversion," *Mechanical Systems and Signal Processing*, vol. 40, no. 1, pp. 356–376, 2013.

[29] MSC Software Corporation, *MSC Nastran 2010 Quick Reference Guide*, MSC Software Corporation, 2010.

[30] D. R. J. Owen and E. Hinton, *Finite Elements in Plasticity*, Pineridge Press, 1980.

[31] C. S. Desai, M. M. Zaman, J. G. Lightner, and H. J. Siriwardane, "Thin-layer element for interfaces and and joints," *International Journal for Numerical and Analytical Methods in Geomechanics*, vol. 8, no. 1, pp. 19–43, 1984.